Author Manuscript

Title: Intensified biobutanol recovery using zeolites with complementary selectivity

Authors: Stijn Van der Perre, Ph.D; Pierre Gelin; Benjamin Claessens; Ana Martin-Calvo, Ph.D; Julien Cousin Saint Remi, Ph.D; Tim Duerinck, Ph.D; Gino V. Baron, Ph.D; Miguel Palomino, Ph.D; Ledys Y. Sanchez; Susana Valencia, Ph.D; Jin Shang, Ph.D; Ranjeet Singh, Ph.D; Paul A. Webley, Ph.D; Fernando Rey, Ph.D; Joeri F.M. Denayer, Ph.D

Intensified biobutanol recovery using zeolites with complementary selectivity

Stijn Van der Perre,[a] Pierre Gelin,[a] Benjamin Claessens,[a] Ana Martin-Calvo,[a] Julien Cousin Saint Remi,[a] Tim Duerinck,[a] Gino V. Baron,[a] Miguel Palomino,[b] Ledys Y. Sánchez,[b] Susana Valencia,[b] Jin Shang,[c] Ranjeet Singh,[d] Paul A. Webley,[d] Fernando Rey,[b] Joeri F.M. Denayer*[a]

Abstract: A vapor phase adsorptive recovery process is proposed as an alternative way to isolate biobutanol from acetone-butanol-ethanol (ABE) fermentation media, offering several advantages compared to liquid phase separation. The effect of water, which is still present in large quantities in vapor phase, on the adsorption of the organics could be minimized by using hydrophobic zeolites. Shape selective all-silica zeolites CHA and LTA were prepared and evaluated via single component isotherms and breakthrough experiments. These zeolites show an opposite selectivity; adsorption of ethanol was favorable on all-silica CHA, while the LTA topology had clear preference for butanol. The molecular sieving properties of both zeolites allowed to easily eliminate acetone from the mixture. The molecular interaction mechanisms were studied by density functional theory (DFT) simulations. Effect of mixture composition, humidity and total pressure of the vapor stream on the selectivity and separation behavior was investigated. Desorption profiles were studied to maximize butanol purity and recovery. The combination of LTA with CHA type zeolites (Si-CHA or SAPO-34) in sequential adsorption columns with alternating adsorption and desorption steps allows to obtain butanol in unpreceded purity and recovery. A butanol purity of 99.7 mole% could be obtained at nearly complete butanol recovery, demonstrating the effectiveness of this technique for biobutanol separation processes.

Introduction

The production of biobutanol from the fermentation of renewable feedstocks (biomass) has received considerable attention as a sustainable and more environmentally-friendly alternative for petroleum based fuels and chemicals.[1] Besides being an excellent biofuel, butanol also serves an important platform molecule to provide mainstream industrial chemicals (butadiene, butyl acrylate, dibutyl ether, tributyl citrate etc.), leading to the production of several high-value products, such as plasticizers, solvents, polymers, coatings, paints ….[2-3] Biobutanol, also referred to as *n*-butanol or 1-butanol, is produced in the acetone-butanol-ethanol (ABE) fermentation process. The most widely used microorganisms for ABE fermentation are anaerobic bacteria, such as the solventogenic *Clostridia* strain including *Clostridium acetobutylicum* and *Clostridium beijerinckii*.[4-5] The ABE fermentation results in a mixture composition of acetone-butanol-ethanol in a 3:6:1 ratio with a total product concentration between 2-3 wt% diluted in water.[6] A downstream process to recover butanol during fermentation must be implemented to reduce product inhibition by butanol itself and prolong the fermentation. However, the low concentration of butanol makes the product separation process highly costly. Conventional distillation processes for the recovery of biobutanol from an ABE fermentation broth require more energy than the energy content of butanol itself.[5-7] Therefore, it is essential to explore other and more efficient separation methods to become competitive and economically viable.[8] In this context, adsorption-based recovery operations are considered as the most promising alternative compared to other methods, like gas stripping, pervaporation and liquid-liquid extractions.[5,9-10] Several researchers studied the adsorptive separation of butanol from fermentation media or from aqueous model solutions.[6,10-24] A wide range of different adsorbent materials were tested and studied, including active carbons,[6,12,22,24] polymeric resins,[6,10-13] zeolites[6,10-11,14-16,18-19,22-23,25] and metal-organic frameworks (MOFs).[20] Cousin Saint Remi et al.[21] developed a conceptual separation process for the recovery and purification of biobutanol by several adsorption steps. García and coworkers[26] studied the column dynamics of an adsorption-drying-desorption process for butanol recovery with silicalite pellets, supported by theoretical models to make a real estimation of the energy requirement of the whole separation process. All of these studies considered adsorption processes in liquid phase conditions.

Nevertheless, about 50% (w/w) of the fermented sugars are converted to the gases CO_2 and H_2 and 33-39% to solvents during the ABE fermentation.[27] This large gas production causes the entrainment of solvent molecules in the vapor phase, resulting in a significant amount of water, butanol, acetone and, to a lesser extent, ethanol in the headspace of the fermenter chamber. This opens perspectives for the recovery of these valuable chemicals from the vapor phase, instead of the liquid phase. Another possibility to enrich the vapor phase with solvents is gas stripping. A combination of gas stripping and adsorption was recently suggested as a promising method for the recovery of butanol from vapor phase.[28-30] At the same time, operation in vapor phase offers several advantages: (1) ABE

[a]   Dr. S. Van der Perre, P. Gelin, B. Claessens, Dr. A. Martin-Calvo, Dr. J. Cousin Saint Remi, Dr. T. Duerinck, Prof. G. V. Baron, Prof. J.F.M. Denayer
       Department of Chemical Engineering
       Vrije Universiteit Brussel
       Pleinlaan 2, 1050 Brussels (Belgium)
       E-mail: Joeri.Denayer@vub.ac.be
[b]   Dr. M. Palomino, L.Y. Sánchez, Dr. S. Valencia, Prof. F. Rey
       Instituto de Tecnologia Quimica
       Universitat Politècnica de València - Consejo Superior de Investigaciones Científicas
       Avenida de los Naranjos, s/n, Valencia, 46022 (Spain)
[c]   Dr. J. Shang
       School of Energy and Environment
       City University of Hong Kong
       Tat Chee Avenue, Kowloon, Hong Kong SAR (P.R. China)
[d]   Dr. R. Singh, Prof. P.A. Webley
       Chemical and Biomolecular Engineering
       The University of Melbourne
       Melbourne, 3010 (Australia)

       Supporting information for this article is given via a link at the end of the document.

concentrations relative to water are higher in vapor phase;[30] (2) less competition effects occur due to absence of acids and fermentable carbohydrates in the vapor phase; (3) adsorbents suffer less from stability issues, like aqueous conditions and low pH (acetic and butyric acid are formed during the fermentation); and (4) clogging or fouling problems due to microbial cells or inorganic salts are avoided.[31]

A critical issue in the adsorptive recovery of butanol is the development or identification of suitable adsorbents. The hydrophilic nature of common types of zeolites makes them inadequate in the presence of large amounts of water vapor.[32] On the contrary, it could be expected that hydrophobic high-silica and all-silica zeolites could allow the selective uptake of butanol in vapor phase, but adsorption data in these conditions are scarce.[8,18,32-33] In that respect, only MFI-type zeolites, such as silicalite-1 (the pure silica analogue of ZSM-5)[8] and high-silica ZSM-5,[33] were tested as adsorbents for the separation of butanol/water vapor mixtures in the form of zeolitic membranes.

In the present study, a new and alternative strategy for the recovery of biobutanol is presented. An approach in which adsorbents with complementary selectivity are combined in a process with separate adsorption columns operating in sequential mode is proposed. Therefore, two hydrophobic zeolites, all-silica LTA (Si-LTA) and all-silica CHA (Si-CHA) (figure 1), were synthesized and studied as selective adsorbents for butanol separation from ABE model solutions in vapor phase. Until now, only the separation of small gasses and light hydrocarbons[34-39] and diffusion of such molecules[39-41] on these pure silica structures was investigated. More importantly, water adsorption experiments on Si-LTA (or ITQ-29), the pure-silica analogue of zeolite A developed by Corma et al.,[42] indicated a very hydrophobic character with a water capacity of only 1 wt% (or 0.55 mmol g^{-1}) at 20 mbar. The CHA zeolite topology on the other hand shows very specific and unusual selectivity for short chain molecules,[43-46] which makes it an interesting material for the separation of short alcohols. A Si-CHA sample, prepared by Miyamoto et al.,[36] showed hydrophobic behavior and revealed a water uptake of about 3.1 mmol g^{-1} at 67 mbar ($P/P_0 = 0.9$).

Adsorption characteristics were determined via vapor phase adsorption isotherms of the most important components present in the head space of the fermenter (acetone, butanol, ethanol and water). Then, separation performance was tested in dynamic conditions by performing vapor phase multicomponent breakthrough experiments, where the effect of composition, humidity of the vapor stream, contact time and total pressure on selectivity was investigated. Finally, the desorption process has been examined with the purpose to obtain a high-purity butanol stream by combining two columns with different adsorbents to allow a high degree of butanol purification at high recovery.
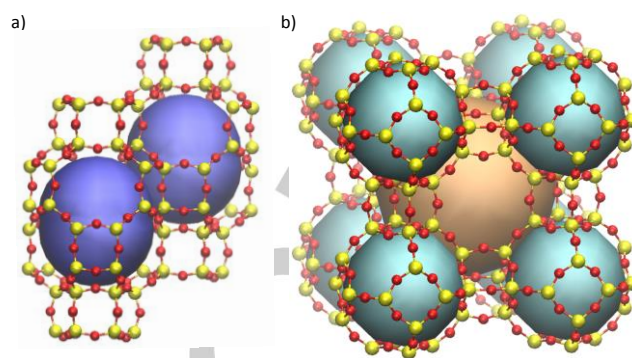

Figure 1. The structural framework of (a) CHA and (b) LTA-type zeolites. Color scheme: red: O; yellow: Si. The colored spheres represent the cavities inside the structure.

Results and Discussion

The aim of the current work is the vapor phase recovery of biobutanol from ABE fermentation solutions via a multicolumn separation process. The concept consists of a 2-step separation (butanol concentration followed by deep purification) with two different adsorption columns in series, containing adsorbents with a complementary selectivity (scheme 1). In a first step, the bulk separation of n-butanol from a diluted humid ABE vapor mixture takes place on an adsorption column containing a hydrophobic adsorbent. At this stage, mainly butanol is adsorbed and an excess of water vapor and other side-products (acetone and ethanol) elute from the column. Subsequently, butanol is desorbed from this first column and then passed over a second column for further purification. In this final step, the remaining traces of side-products and water still present in the enriched butanol stream are adsorbed to obtain a very pure biobutanol stream at maximal recovery.
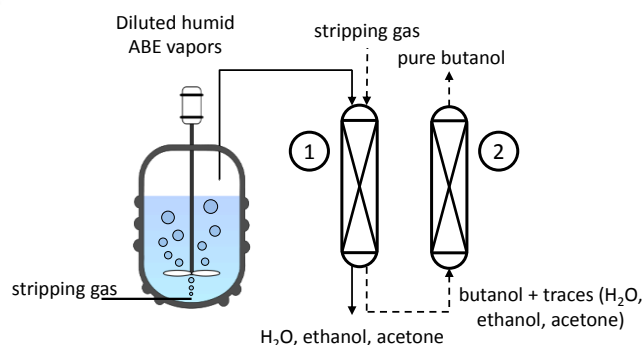
Scheme 1. Combined adsorption-desorption process for the recovery and purification of butanol from the head space in the ABE fermentation process. Step 1: head space vapors from fermenter are lead to the first adsorption column for bulk separation (solid line): adsorption of butanol in column 1. Step 2: the effluent of column 1, obtained during desorption of column 1, is lead to column 2 for purification and removal of impurities. All components are obtained in a dilute stream in the stripping gas.

Vapor phase adsorption of individual ABE components

Single component adsorption isotherms of butanol, ethanol and water are shown in figure 2 for both materials. Interestingly, acetone was barely adsorbed because its kinetic diameter (4.7 Å) is larger than the CHA (3.8 x 4.2 Å) and LTA cage (4.2 x 4.2 Å) windows (figure S5).[47] ==This results in an extremely slow uptake and can be perceived as a molecular sieving property of both zeolites for this molecule, which makes the separation task much easier since acetone can be removed from the mixture in one step without interference with the other mixture compounds.==
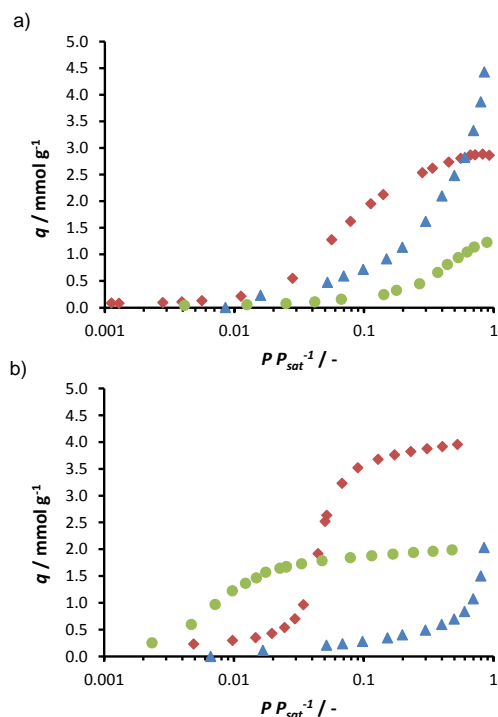

a)

b)

Figure 2. Vapor phase adsorption isotherms of ethanol (◊), *n*-butanol (○) and water (△) on (a) Si-CHA and (b) Si-LTA at 40 °C. The butanol isotherm on Si-CHA is not in equilibrium despite an equilibrium time of about 420 min.

Generally, the adsorption capacities of Si-LTA are larger than those of Si-CHA, due to better packing of molecules in the spherical and larger cages of the LTA structure (11.4 Å) than in the ellipsoidal and smaller CHA cages (6.7 x 10 Å). As follows from Ar porosimetry, both materials possess very similar micropore volumes; 0.27 and 0.29 ml g^{-1} for Si-CHA and Si-LTA, respectively, corresponding very well with literature values.[34,48]

It should be noted that Si-LTA and Si-CHA show an opposite affinity for ethanol and butanol at low vapor pressure. Si-CHA prefers to adsorb the smallest alcohol, ethanol, over the complete pressure range, while Si-LTA shows a larger affinity for butanol at low pressure. On Si-CHA, butanol uptake is kinetically limited and very slow, as shown in figure 3a. Therefore, two pseudo-adsorption isotherms were measured with a different equilibrium time of 180 and 420 min. respectively, but even after 420 min., equilibrium was not fully reached, pointing at very slow intra-particle diffusion (figure 3b). This behavior is well-known for

the CHA structure.[49] A drastic decrease in molecular diffusivity is observed once the adsorbate size [50] becomes comparable to the size of the small zeolite cage (6.7 x 10 Å). Additionally, Daems *et al.*[43] found that shorter alcohols such as ethanol, which can adsorb with their main carbon chain perpendicularly to the length axis of the cage, are much more efficiently packed than longer alcohols, resulting in an entropic advantage and larger affinity for the shorter chains. The combination of these kinetic and entropic effects results in a strong and unusual preference for ethanol over butanol on Si-CHA. Both phenomena are absent on Si-LTA with its larger cages, allowing adsorption of much longer chains as compared to Si-CHA. Its ethanol adsorption isotherm is S-shaped while butanol exhibits a classical type I profile, with a higher uptake for butanol in comparison with ethanol in the lower pressure range. Ethanol adsorption sharply increases at a relative pressure of 0.03-0.04 due to adsorbate-adsorbate interactions.
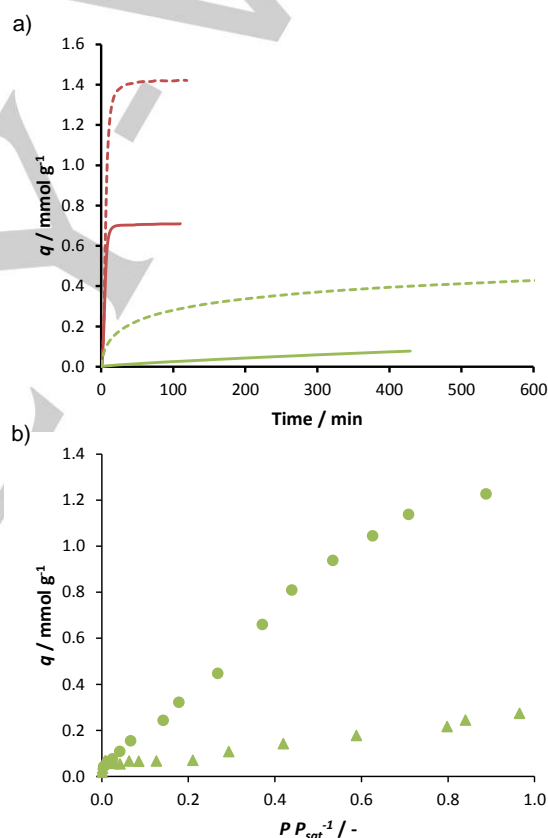

a)

b)

Figure 3. (a) Uptake kinetics of ethanol (red) and *n*-butanol (green) on Si-CHA (solid) and Si-LTA (dashed) at P = 1000 Pa for ethanol and P = 500 Pa for *n*-butanol at 40 °C. (b) Butanol adsorption isotherms with equilibrium time of 180 (△) and 420 min (○) on Si-CHA at 40 °C.

Compared to the alcohols, adsorption of water is low, confirming the hydrophobic nature of these all-silica materials. Especially Si-LTA has a very low affinity for water, with a capacity of less than 0.04 g g^{-1} (or 2.0 mmol g^{-1}) at a relative humidity of 85%. The water uptake of the Si-CHA sample is higher and

corresponds to about 0.08 g g⁻¹ (or 4.4 mmol g⁻¹) at P/P_0 = 0.85. The reason for this less hydrophobic character of Si-CHA can be ascribed to local defects, such as polar silanol groups, which are also found in other pure silica zeolite structures.[51-52] ²⁹Si BD-MAS-NMR spectrum of pure silica CHA zeolite shows the presence of two small resonances at -101 and -102 ppm that can be unambiguously ascribed to silanol groups, since these two signals increase their intensity in the ¹H → ²⁹Si CP-MAS NMR spectrum. On the contrary, there is any signal in the ²⁹Si BD-MAS-NMR spectrum of Si-LTA zeolite, confirming that LTA material is an essentially defect-free pure silica zeolite (figure S4).

DFT calculations indicate that both Si-CHA and Si-LTA have a much stronger affinity to ethanol and butanol than to water, justifying the hydrophobicity of these two zeolites. The interaction energy at very low degree of pore filling follows the order butanol > ethanol > water for both materials (table 1). This confirms that the selectivity towards ethanol of Si-CHA is a result of kinetic restrictions and steric effects. The higher (∼5 kJ mol⁻¹) adsorption energies for Si-CHA in comparison with Si-LTA can be attributed to the smaller size and specific shape of the chabazite cage, resulting in stronger interactions.

Table 1. "zero-loading" interaction energy[a] (kJ mol⁻¹) on a defect-free Si-CHA and Si-LTA at 0 K.

	"zero-loading" interaction energy [kJ mol⁻¹]	
	Si-CHA	Si-LTA
ethanol	-46.83	-41.68
butanol	-70.85	-64.63
water	-25.60	-25.04

[a] The "zero-loading" interaction energy is defined as the adsorption energy at a loading of one molecule adsorbed per supercage, reflecting the intrinsic interaction between adsorbate and adsorbent.

In both structures, ethanol and butanol prefer to adsorb close to the center of the hydrophobic cages, maximizing their interactions, while water prefers sitting around the eight-membered ring, as illustrated in figure 4. DFT calculations also demonstrate that the adsorption interaction energy per ethanol molecule becomes more negative with loading on Si-LTA, suggesting ethanol-ethanol interactions become increasingly important with loading (figure 5). This effect can be perceived in the adsorption isotherm of ethanol on Si-LTA, where the sigmoidal shape points at a cooperative adsorption mechanism. On Si-CHA, a strong decrease in interaction energy (from -46.8 to -60.4 kJ mol⁻¹) is observed for the second molecule, probably due to a better confinement. Beyond 3 ethanol molecules per CHA cage, the interaction energy per ethanol molecule becomes less negative. This reveals unfavorable interactions among the ethanol molecules. To further prove this point, the intermolecular interaction energies between ethanol molecules are calculated

by removing the LTA and CHA structure and fixing the original adsorption configurations of the adsorbed ethanol molecules. The positive interaction energy values in the case of Si-CHA (figure 5), indicate that ethanol-ethanol interactions are unfavorable in this configuration, whereas negative energy values are found for Si-LTA. The large difference in adsorption behavior between Si-CHA and Si-LTA is related to the different shape of the supercage, with a much larger degree of sterical hindering in Si-CHA.
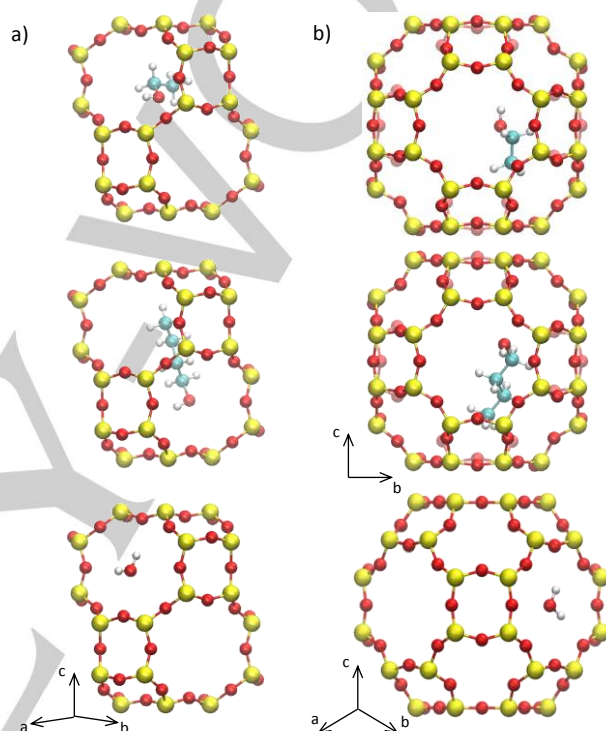

Figure 4. Preferred location sites of ethanol (top), butanol (middle) and water (bottom) in the (a) Si-CHA and (b) Si-LTA structure. Water molecule in the LTA cage is located in the plane of the eight-membered window. Color scheme: red: O; cyan: C; white: H; yellow: Si.
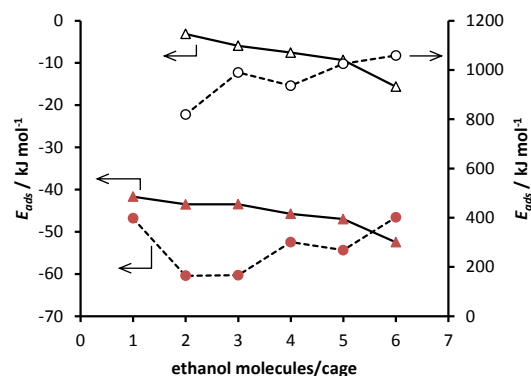

Figure 5. Adsorption interaction energy per ethanol molecule as function of the ethanol loading in the Si-CHA (closed circles) and Si-LTA (closed triangles) cage and without the zeolite structure while fixing the original adsorption configurations of the ethanol molecules (open symbols).

1-column vapor phase separation of ABE components

In a first stage, the separation of ethanol/butanol mixtures in vapor phase conditions, in absence of water and acetone, was investigated by performing breakthrough experiments using one single column containing one of both materials. Separation of ethanol and butanol is achieved with a clear difference in breakthrough time on both adsorbents (figure 6). It should be noted that Si-LTA and Si-CHA show an opposite selectivity (figure 6a-b). Si-CHA prefers to adsorb ethanol and almost fully excludes butanol, resulting in an instantaneous breakthrough of butanol and strong retention of ethanol. Si-LTA on the other hand has a clear preference for butanol. The ethanol breakthrough profile of Si-LTA shows a large roll-up, indicating that butanol displaces all adsorbed ethanol. The unusual shape of the ethanol breakthrough profile originates from the sigmoidal shape of its adsorption isotherm.[53] The effect of ethanol/butanol mixture composition and pressure on the separation performance is shown in Supporting Information (figure S8).
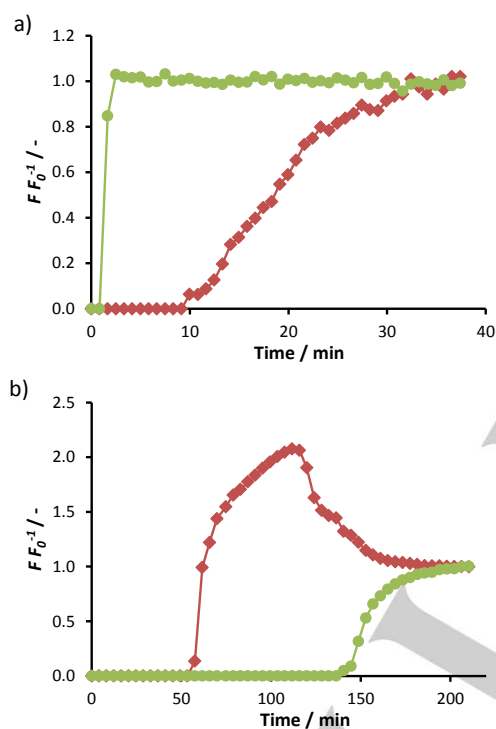

Figure 6. Breakthrough curves of an equimolar ethanol (◊)/butanol (○) vapor mixture (P_{tot} = 1000 Pa) on (a) Si-CHA and (b) Si-LTA with a total flow rate of 10.5 Nml min^{-1} at 40 °C.

Effect of water Since the ABE fermentation process is performed in water, a gas stream obtained by stripping the liquid phase contains a large amount of water vapor. It is well known that the presence of water vapor negatively affects the separation performance of most adsorbents. The influence of water vapor was therefore tested in dynamic conditions. Even at high relative humidity, the selectivity between ethanol and butanol was preserved in both cases (figure 7a,b). No loss in

ethanol/butanol selectivity was observed in presence of water vapor for Si-CHA compared to the dry ethanol/butanol mixture (figure 7c). At low water concentrations (x_{water} = 0.25 or RH = 7%), the selectivity increases even with a factor 2, because the decrease in butanol capacity is relatively larger than that of ethanol. At higher concentrations (from x_{water} = 0.50 or RH = 21% on), a downward trend in the ethanol/butanol selectivity is discernable. For Si-LTA on the other hand, a negative effect of water vapor on the butanol/ethanol selectivity is noticed. While the butanol capacity is nearly unaffected by water vapor, the presence of only few adsorbed water molecules in the pores makes the material less hydrophobic which results in a larger affinity for the more polar alcohol, ethanol (figure 7d). Also, hydrogen bonding effects (between ethanol and adsorbed water molecules) might play an important role in the attraction of ethanol, leading to higher uptakes of ethanol.[54] This results in a strong decrease of the selectivity (from 37 to 7) once water is added to the structure. Nevertheless, separation of butanol and ethanol is still achieved.

ABE mixture separation In a next step, the separation of a model vapor mixture (see SI) with approximately the same composition as in the head space of a fermentation chamber was evaluated for both hydrophobic zeolites. The ABE components were present in a 4:6:1 ratio, with a water mole fraction of 90% (or a relative humidity of about 60%) in the vapor phase. As the ABE components are present in low concentrations in a real fermentation medium (table S2), the partial pressures of these compounds in the feed are located in the low-pressure regime of the isotherms (figure S9). Resulting breakthrough profiles are shown in figure 8. The water profiles were omitted for clarity. Acetone shows immediate breakthrough, since it is too large to enter the pores of both materials and thus elutes from the columns without being adsorbed. Although a significant amount of water is adsorbed in the present conditions of low concentration of the ABE components (table 2), both materials maintain their separation ability. Again, a clear preference for ethanol was observed on Si-CHA, while Si-LTA showed strong retention of butanol (figure 8). While Si-CHA allows to selectively remove ethanol from an ABE fermentation medium, Si-LTA appears to be very effective for the isolation of biobutanol from the same mixture. As a consequence of its shape selective properties in combination with its hydrophobic character, Si-LTA is an interesting candidate for biobutanol recovery.

Table 2. Adsorption capacities obtained in breakthrough experiments with a humidified ABE mixture on Si-CHA and Si-LTA at 40 °C.

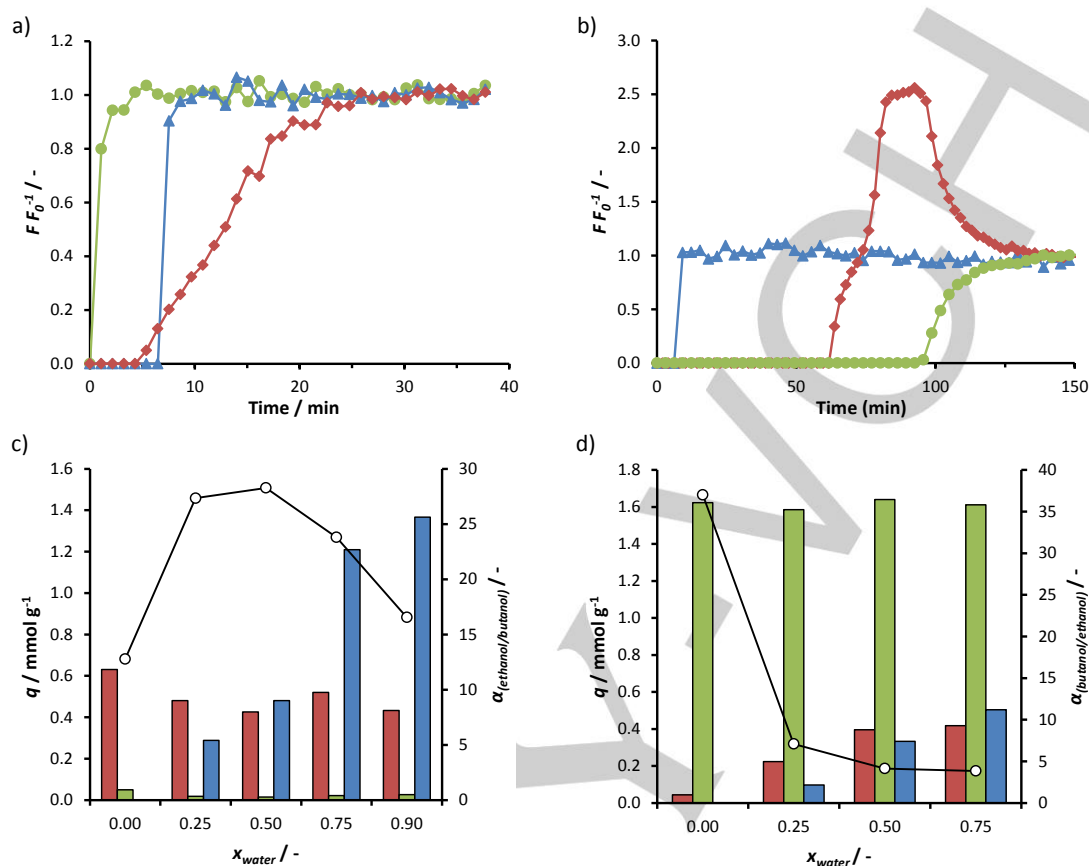| q [mmol g^{-1}]	Si-CHA	Si-LTA
water	1.288	0.629
acetone	0.004	0.006
butanol	0.029	1.458
ethanol	0.112	0.060

Figure 7. Breakthrough profiles of an ethanol (◊)/butanol (○)/water (Δ) vapor mixture on (a) Si-CHA and (b) Si-LTA with a total flow rate of 10.5 Nml min^{-1} at 40 °C. Mixture composition: $P_{ethanol}$ = 750 Pa, $P_{butanol}$ = 750 Pa and P_{water} = 1500 Pa (x_{water} = 0.5). Adsorption capacities (bars: ethanol = red; butanol = green; water = blue) and selectivity (line graph) as function of the mole fraction of water (x_{water}) for different ethanol/butanol/water mixtures on (c) Si-CHA and (d) Si-LTA at 40 °C. Ethanol and butanol are always in a 1:1 molar ratio. The water mole fraction is based on the total hydrocarbon and water fraction in the vapor phase (relative humidity varies from 6 to 66%).
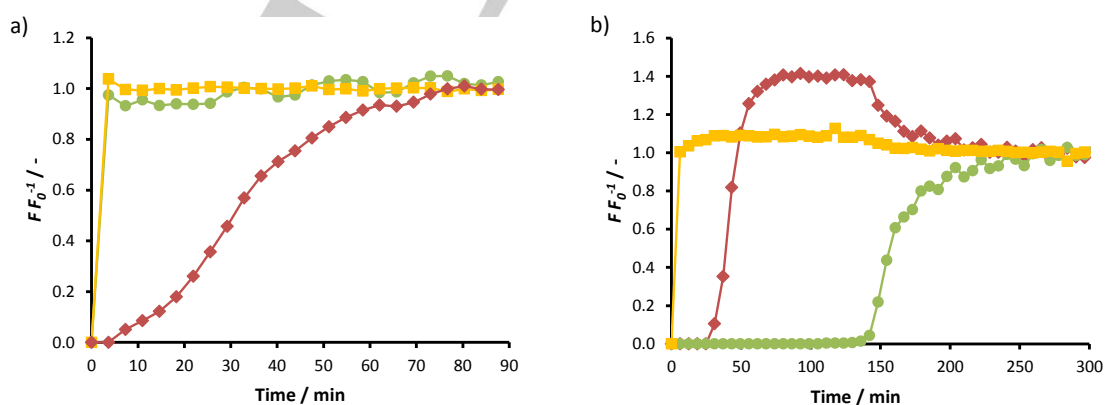

Figure 8. Breakthrough profiles of an acetone (□)/ethanol (◊)/butanol (○)/water mixture on (a) Si-CHA and (b) Si-LTA with a total flow rate of 14.5 Nml min^{-1} at 40 °C. The water profile is omitted for clarity. Composition: $P_{acetone}$ = 192 Pa, $P_{ethanol}$ = 50 Pa, $P_{butanol}$ = 299 Pa and P_{water} = 4220 Pa (x_{water} = 0.89).
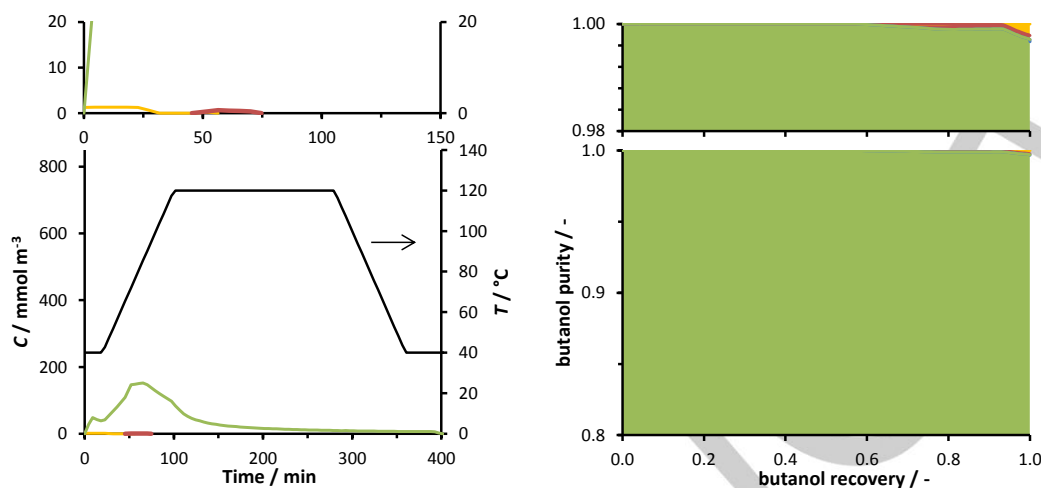
Figure 9. Desorption profiles of acetone (yellow), butanol (green), ethanol (red), and water (blue) and temperature profile (black) of a Si-LTA column in combination with SAPO-34 (50 min) (left) and the corresponding purity-recovery plot of butanol (right). Purity and recovery are expressed on a mole basis. The areas represent the relative amount of the components in the outlet stream: acetone (yellow), butanol (green), ethanol (red) and water (blue). The second adsorption column is kept at a temperature of 40 °C. A zoom-in of both graphs is provided above the full scale charts. No water signal was detected in this configuration.

1-step butanol recovery During the adsorption step, Si-LTA is contacted with the feed vapor mixture, mainly resulting in the uptake of butanol, but also in the adsorption of a significant amount of water, a small amount of ethanol and traces of acetone. In order to recover the adsorbed butanol from the Si-LTA pores, a desorption step is required.

In a first approach, the Si-LTA column was flushed with an inert gas and subjected to a temperature increase (T_{max} = 120 °C) to cause desorption. Initially, a relatively high butanol product could be obtained (figure S10). Starting from a butanol recovery of about 60%, purity starts to decrease due the presence of traces of acetone (negligible) and ethanol. Above a recovery of 95%, close to complete butanol recovery, a significant decrease in the purity is observed due to the presence of significant amounts of water in the column effluent (figure S10).

2-column vapor phase separation of ABE components

In order to increase the butanol purity at high recovery, the effluent of the Si-LTA column produced during the desorption step was directly sent to a second column to trap the most important impurities, as shown in scheme 2. Chabazite zeolite, with its selectivity complementary to that of Si-LTA and unique capability of rejecting butanol, was used to selectively trap ethanol without adsorbing butanol, which would otherwise result in a loss in recovery. Two different materials with the CHA zeolite topology were tested as second adsorbent. The hydrophobic Si-CHA material was selected for its very large selectivity towards ethanol while the hydrophilic SAPO-34 material was studied since it combines large ethanol selectivity[45-46] with good water adsorption properties (figure S6).
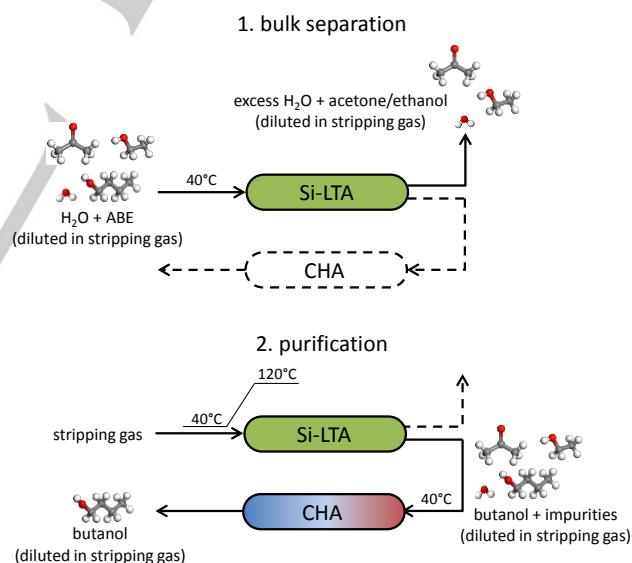
Scheme 2. Overview of the 2-step butanol recovery configuration, consisting of two columns with different selectivity. Solid lines indicate the active flow; dotted lines indicate the inactive flow.

A fixed operation time was used for the second column, about 50 min. from the start of the desorption step, yielding a substantial improvement compared to the 1-step butanol recovery system (figure S11b). After this period, the outlet stream of the LTA column contained nearly pure butanol as all

impurities already desorbed (figure S10), and needed no further purification with a second CHA column. The use of the second column during complete desorption of the Si-LTA column resulted in suboptimal performance (table 3), as discussed in Supporting Information (figure S11a). During the first 50 min., the Si-CHA column allowed to remove a large fraction of the ethanol impurity from the Si-LTA column effluent, but also resulted in a decrease in water content. As a result, a significant increase in butanol purity was observed at high butanol recovery. Only above a butanol recovery of 99%, butanol purity decreased below 96% (figure S11b).

Nevertheless, the highest purities were obtained with SAPO-34, a hydrophilic chabazite type zeolite, as second adsorbent. This material removed all water and a large part of the ethanol present in the Si-LTA effluent. The desorption profile obtained with this configuration was converted into a purity-recovery plot. (figure 9). The purity of butanol at the column outlet is plotted as a function of the recovery of butanol, starting from the end of the desorption curve and then moving up to the first release of butanol. So the last point in the desorption profile is taken at zero recovery, and the first point at full recovery. With this combination of adsorbents, butanol purity was exceeding 99%, even at butanol recovery close to 100% (table 3). When using SAPO-34 to purify the effluent of the Si-LTA column, traces (< 0.25 wt%) of other impurities were found in the product stream. The catalytic activity of SAPO-34 with regard to small alcohols is well-known;[55] SAPO-34 is often used as a catalyst in the methanol-to-olefin process (MTO),[56] but also in ethanol-to-olefin (ETO)[57] and even acetone-to-olefin (ATO)[58] processes, which usually take place at high temperatures (>350 °C). At lower temperatures, SAPO-34 demonstrates only a reduced catalytic activity.[55,59-61] Since adsorption took place at 40 °C, only an insignificant amount of catalytic products was formed (see SI). The main product of ethanol conversion on SAPO-34 is ethylene, together with some byproducts as diethyl ether, acetaldehyde, and propylene.[57,61] Acetone can be converted into isobutene and also, to a much smaller degree, in other hydrocarbons such as ethylene, propylene, and C_1–C_4 saturated alkanes where the reaction proceeds mainly on the outer surface of SAPO-34 crystals.[58] The identification of these products was beyond the scope of this work.

Table 3 summarizes the results obtained with a second adsorption column during desorption of the Si-LTA column for different levels of butanol recovery (90%, 95%, 99%, >99.5%). The use of a second column with complementary selectivity generates a manifest increase in the biobutanol purity at the different recovery levels. At >99.5% recovery, a limited decrease in purity can be observed for the CHA column, because a small part of the butanol is adsorbed by Si-CHA despite the kinetic limitations on the chabazite structure. The hydrophilic SAPO-34 zeolite allowed to reach significantly higher purities than the more hydrophobic Si-CHA zeolite, because of its higher water affinity[62] (figure S6a). The combination of Si-LTA and SAPO-34 led to a final butanol purity of 99.9 wt% (or 99.7 mole%, see table 3) whilst recovering all of the desorbing butanol. These

values are high compared to butanol purity values found in the literature. Faisal et al.[63], for instance, performed adsorption in liquid phase on a silicalite adsorbent, but desorbed using nitrogen gas. The product stream resulting from desorption was subsequently sent to a condenser, with the maximal butanol purity reported to be 88.5 wt%. Liquid phase desorption results of Cousin-Saint-Remi et al.[20] on ZIF-8 showed a maximum butanol concentration of 20 wt% using methanol as displacement liquid. Abdehagh et al.[24] used a similar approach as Faisal et al.[63] on their activated carbon material F-400, first performing adsorption of an ABE model mixture in liquid phase, followed by desorption using CO_2 as carrier gas. In their study, a final concentration of 15 wt% was reported.[24] This approach was also used by Saravanan et al.[64] on ZSM-5. Inert argon was used as purging gas, yielding a maximal butanol concentration of 84.3 wt%. Similarly, Lin et al.[65] observed a final butanol concentration of 14 wt% using methanol as desorbing agent after liquid phase adsorption of an ABE model mixture. Águeda et al.[26] proposed a butanol recovery process using silicalite pellets wherein a purity of 98 wt% could be obtained from dilute aqueous solutions (0.5-2 wt%) with a recovery of 60-70 wt%. In this context, it should be mentioned that a butanol purity of 76 wt% (or 65.5 mole%) could be achieved on the Si-LTA column without combining it with a second adsorption column and recovering all of the desorbing butanol.

Table 3. Butanol purity (mole%) at different levels of recovery (%) for different multicolumn experiments with Si-LTA.

	purity [mole%]			
recovery [%]	Si-LTA	Si-LTA + Si-CHA[a]	Si-LTA + Si-CHA (50 min)[b]	Si-LTA + SAPO-34 (50 min)[b]
>99.5	65.5	64.6	66.0	99.7
99	70.6	68.7	96.1	99.7
95	98.8	96.3	99.5	99.8
90	99.4	98.7	99.6	99.9

[a] Second column is used during the complete desorption process. [b] Second column is used during the first 50 minutes of the desorption process.

Conclusions

Two all-silica zeolites, Si-CHA and Si-LTA, were synthesized and identified for the adsorptive recovery of bioalcohols from an ABE model mixture in the presence of water vapor. The effect of water on the adsorption of the organics was limited, because of the hydrophobic nature of these zeolites. Si-CHA and Si-LTA displayed a complementary selectivity; Si-CHA preferred ethanol, while Si-LTA showed very interesting properties for biobutanol recovery. The combination of both complementary materials in sequential columns with alternating desorption and adsorption steps was proposed to obtain butanol in very high purity and

recovery. A butanol purity larger than 99.5% could be obtained at a recovery > 99% using a combination of Si-LTA column and SAPO-34, the polar analogue of Si-CHA, as second column.

The results presented herein illustrate the potential of hydrophobic and shape selective zeolites in the adsorptive recovery of bioalcohols, in particular biobutanol, from ABE fermentation mixtures. This approach in which adsorbents with complementary selectivity are combined could be used to obtain all mixture compounds in high purity or extended to the separation and/or isolation of other, rather small, biobased components from aqueous mixtures in vapor/liquid phase.

Experimental Section

Synthesis Pure silica chabazite (Si-CHA) was synthesized by following a reported procedure.[48] This procedure features a hydrothermal synthesis process using *N,N,N*-trimethyladamantammonium hydroxide (TMAdaOH) as the structure-directing agent in the presence of fluoride at near to neutral pH. In a typical synthesis 13.00 g of tetraethylorthosilicate were firstly hydrolyzed in 31.18 g of a 1.0 M TMAdaOH aqueous solution. Then the mixture was stirred using a magnetic stirrer to allow the ethanol and water to evaporate to a final H_2O/SiO_2 molar ratio of 3.0. After that, 1.33 g of HF (aq., 46.9%) was added and the mixture was homogenized by hand using a stainless steel spatula prior to being transferred to a Teflon lined stainless steel autoclave of 60 ml in volume. The autoclave was heated at 150 °C while rotated at 60 rpm in an oven. After crystallization for 40 h (pH = 8.5) the solid product was collected, washed with deionized water, and dried in a vacuum oven at 80 °C.

Pure silica LTA (Si-LTA), also named as ITQ-29, was synthesized in fluoride medium at 135 °C for 5 days using 4-methyl-2,3,6,7-tetrahydro-1H,5H-pyrido[3.2.1-ij] quinolinium (ROH) and tetramethylammonium (TMAOH) hydroxides as organic structure directing agents from a gel of molar composition: SiO_2 : 0.25 ROH : 0.25 TMAOH : 0.5 HF : 3 H_2O. 5 wt% of the silica was added as seeds of pure Si-LTA for promoting zeolite crystallization. The solid was recovered by filtration and extensively washed with distilled water and dried at 100 °C, overnight. The occluded organic was removed by aerial calcination at 700 °C during 6 hours.

Commercial SAPO-34 was obtained from ACS Material (Medford, USA) and was already extensively characterized in a previous study.[66] The obtained crystals of Si-CHA and Si-LTA have an average diameter of around 6 and 2.5 μm respectively.

Characterization Ar porosimetry measurements were performed on an Autosorb AS-1 (Quantachrome instruments) device at 87 K. Both samples were activated at 350 °C under vacuum for at least 3 h. Pore volumes were determined at a relative pressure of around 0.2, while pore size distributions were determined via Density Functional Theory (DFT) using non-local DFT (NLDFT) parameters for zeolites/silica, assuming cylindrical and/or spherical pores (figure S1).

X-ray powder diffraction (XRPD) data were collected at ambient conditions using a Panalytical X'Pert PRO diffractometer with capillary geometry, using an hybrid monochromator for CuKα_1 radiation (λ_1=1.5406), divergence slit: fixed = ¼°; goniometer arm length: 240 mm; detector: Panalytical X'Celerator; tube voltage and intensity: 45 kV, 40

mA; scan range: 3.0° to 75.0° (2θ), scan step size: 0.017° (2θ); counting time: 2440 s/step. For measurement, the sample was placed in a 0.7 mm diameter sealed glass capillary. The XRPD results (figure S2) demonstrate the crystallinity of the synthesized materials.

^{29}Si NMR spectra were recorded in a Bruker AV-400WB spectrometer using a BL7mm probe, spinning at 5 Khz. ^{29}Si Bloch decay (BD)-MAS NMR spectra were measured using pulses of 4 ms corresponding to a flip angle of π/3 radians and recycle delay of 60 s. ^{1}H to ^{29}Si cross polarization (CP)-MAS NMR spectra were measured using π/2 pulse length for ^{1}H of 5 ms, a contact time of 3.5 ms and recycle delay of 3s. Both, ^{29}Si BD-MAS and ^{1}H to ^{29}Si CP-MAS spectra were recorded with proton decoupling (tppm). ^{29}Si NMR spectra were referred to tetramethylsilane (TMS) (0 ppm). During the acquisition of ^{29}Si spectra, the samples were span at the magic angle (MAS) at a rate of 5-5.5 kHz.

Density Functional Theory All results were calculated using the Vienna *ab initio* Simulation Package (VASP) with the projector augmented waves (PAW) approach.[67-68] The cut-off energy of the plane wave basis-set was 405 eV. A gamma point only k-point mesh was used for an extended zeolite structure with infinite repeating unit cells. Such a cut-off energy and k-point mesh were tested to ensure the total energy value convergence within 1 meV atom^{-1}. The atomic positions were optimized with the conjugate gradient method until the forces acting on atoms were below 0.015 eV Å^{-1} and the zeolite structure was allowed to relax. To account for the van der Waals interactions, the calculations were conducted using the DFT-D3 van der Waals interaction correction method with Becke–Jonson damping (IVDW=12).[69] The adsorption interaction energy (0 K) of a given guest molecule is defined as the difference between the total energy of zeolite augmented by the total energy of an isolated guest molecule: $E_{ads} = E_{tot}(zeolite+gas) - E_{tot}(zeolite) - E_{tot}(gas)$.

Vapor phase adsorption experiments Vapor phase isotherms were measured at 40 °C with the gravimetric method on a microbalance of VTI Corporation (SGA-100H). Nitrogen (Air Liquide, >99.998%) bubbling through the reservoir, filled with a liquid adsorbate, entrains the organic vapor (dynamic method). Prior, samples were activated by heating at 350 °C for 2 h under N_2 flow. Some vapor phase isotherms were also measured without carrier gas (static method), using a pressure-controlled method (IGA-002, Hiden Isochema). This method enables one to achieve lower vapor pressures than the dynamic method. Activation was performed here at the same temperature, but under vacuum. It was already shown that both methods yield similar results in their overlapping vapor pressure range.[70]

Vapor phase breakthrough experiments Breakthrough experiments were performed using a column of length 10 cm and internal diameter 0.21 cm, which was packed with zeolite pellets (between 250 and 500 μm). Mixtures of ethanol/butanol, ethanol/butanol/water and acetone/butanol/ethanol/water, diluted in He, were sent through the column at 40 °C. Experiments were performed at different partial pressures of ethanol, butanol and water to study the effect of water and ethanol/butanol composition on the selectivity of Si-CHA and Si-LTA. The gas stream at the outlet of the column was analyzed on-line with a gas chromatograph (GC) equipped with an automatic gas injection valve. A Stabilwax® (crossbond Carbowax-PEG) column (Restek) of length 15 m,

internal diameter 250 µm, and film thickness 0.5 µm was used for the separation of different mixtures. The adsorbed amounts, q_i and q_j, were calculated by integration of the experimental breakthrough curves.[71] An average adsorption selectivity, α, for components i and j, is defined as:

$$\alpha = \frac{q_i}{p_i} \Big/ \frac{q_j}{p_j} \tag{1}$$

Desorption experiments were performed using an inert gas, He, at a flow rate of 10 ml/min where the column was subjected to a specific temperature program (120 °C for 180 min with heating and cooling rate of 1 °C min⁻¹). From these desorption profiles, the purity and recovery of a component i can be calculated. He was not included in the calculation of the purity. A more detailed explanation of the calculation is found in SI.

Author contribution

S.V.d.P., P.G., B.C., A.M-C., J.C.S.R., T.D., G.V.B and J.F.M.D. contributed to the development of the experimental approach and conducted all the adsorption related experiments (Ar porosimetry, isotherms and breakthrough experiments). M.P., L.Y.S., S.V., and F.R. provided the Si-LTA material, while J.S., R.S. and P.A.W. synthesized the Si-CHA material, including the corresponding XRD and SEM characterization of each material, respectively. NMR measurements were realized by the group of F.R. and the DFT calculations were performed by J.S and the group of P.A.W. All authors participated in the writing of the manuscript.

Acknowledgements

[1]   R. Luque, L. Herrero-Davila, J. M. Campelo, J. H. Clark, J. M. Hidalgo, D. Luna, J. M. Marinas, A. A. Romero, *Energy Environ. Sci.* **2008**, *1*, 542-564.

[2]   M. Mascal, *Biofuels, Bioproducts and Biorefining* **2012**, *6*, 483-493.

[3]   F. E. I. Deswarte, *Introduction to chemicals from biomass*, (Eds.: J. H. Clark, F. E. I. Deswarte), John Wiley & Sons, Chichester, **2015**, pp. 130-142.

[4]   P. Dürre, *Biotechnol. J.* **2007**, *2*, 1525-1534.

[5]   N. Abdehagh, F. H. Tezel, J. Thibault, *Biomass and Bioenergy* **2014**, *60*, 222-246.

[6]   H.-J. Huang, S. Ramaswamy, Y. Liu, *Sep. Purif. Technol.* **2014**, *132*, 513-540.

[7]   C. Xue, J. Zhao, C. Lu, S.-T. Yang, F. Bai, I. C. Tang, *Biotechnol. Bioeng.* **2012**, *109*, 2746-2756.

[8]   A. Farzaneh, M. Zhou, E. Potapova, Z. Bacsik, L. Ohlin, A. Holmgren, J. Hedlund, M. Grahn, *Langmuir* **2015**, *31*, 4887-4894.

[9]   A. Oudshoorn, L. A. M. van der Wielen, A. J. J. Straathof, *Ind. Eng. Chem. Res.* **2009**, *48*, 7325-7336.

[10]   N. Qureshi, S. Hughes, I. S. Maddox, M. A. Cotta, *Bioprocess Biosyst. Eng.* **2005**, *27*, 215-222.

[11]   B. M. Ennis, N. Qureshi, I. S. Maddox, *Enzyme Microb. Technol.* **1987**, *9*, 672-675.

[12]   W. J. Groot, K. C. A. M. Luyben, *Appl. Microbiol. Biotechnol.* **1986**, *25*, 29-31.

[13]   L. Nielsen, M. Larsson, O. Holst, B. Mattiasson, *Appl. Microbiol. Biotechnol.* **1988**, *28*, 335-339.

[14]   N. Qureshi, M. M. Meagher, R. W. Hutkins, *J. Membr. Sci.* **1999**, *158*, 115-125.

[15]   J. Huang, M. M. Meagher, *J. Membr. Sci.* **2001**, *192*, 231-242.

[16]   N. Qureshi, M. M. Meagher, J. Huang, R. W. Hutkins, *J. Membr. Sci.* **2001**, *187*, 93-102.

[17]   D. R. Nielsen, K. J. Prather, *Biotechnol. Bioeng.* **2009**, *102*, 811-821.

[18]   A. Oudshoorn, L. A. M. van der Wielen, A. J. J. Straathof, *Biochemical Engineering Journal* **2009**, *48*, 99-103.

[19]   H. Zhou, Y. Su, X. Chen, Y. Wan, *Sep. Purif. Technol.* **2011**, *79*, 375-384.

[20]   J. Cousin Saint Remi, T. Remy, V. Van Hunskerken, S. Van der Perre, T. Duerinck, M. Maes, D. De Vos, E. Gobechiya, C. E. A. Kirschhock, G. V. Baron, J. F. M. Denayer, *Chemsuschem* **2011**, *4*, 1074-1077.

[21]   J. Cousin Saint Remi, G. V. Baron, J. F. M. Denayer, *Adsorpt.-J. Int. Adsorpt. Soc.* **2012**, *18*, 367-373.

[22]   N. Abdehagh, F. H. Tezel, J. Thibault, *Adsorption* **2013**, *19*, 1263-1272.

[23]   A. Faisal, A. Zarebska, P. Saremi, D. Korelskiy, L. Ohlin, U. Rova, J. Hedlund, M. Grahn, *Adsorption* **2014**, *20*, 465-470.

[24]   N. Abdehagh, P. Gurnani, F. H. Tezel, J. Thibault, *Adsorption* **2015**, *21*, 185-194.

[25]   R. F. DeJaco, P. Bai, M. Tsapatsis, J. I. Siepmann, *Langmuir* **2016**, *32*, 2093-2101.

[26]   V. I. Águeda, J. A. Delgado, M. A. Uguina, J. L. Sotelo, Á. García, *Sep. Purif. Technol.* **2013**, *104*, 307-321.

[27]   V. V. Zverlov, O. Berezina, G. A. Velikodvorskaya, W. H. Schwarz, *Appl. Microbiol. Biotechnol.* **2006**, *71*, 587-597.

[28]   Y. Cao, K. Wang, X. Wang, Z. Gu, W. Gibbons, H. Vu, *Appl. Surf. Sci.* **2015**, *349*, 1-7.

[29]   Y. Cao, K. Wang, X. Wang, Z. Gu, W. Gibbons, H. Vu, *Bioresour. Technol.* **2015**, *196*, 525-532.

[30]   N. Abdehagh, B. Dai, J. Thibault, F. Handan Tezel, *Journal of Chemical Technology & Biotechnology* **2017**, *92*, 245-251.

[31]   T. Ezeji, C. Milne, N. D. Price, H. P. Blaschek, *Appl. Microbiol. Biotechnol.* **2010**, *85*, 1697-1712.

[32]   Y. Takeuchi, H. Iwamoto, N. Miyata, S. Asano, M. Harada, *Separations Technology* **1995**, *5*, 23-34.

[33]   H. Zhou, D. Korelskiy, E. Sjöberg, J. Hedlund, *Microporous Mesoporous Mater.* **2014**, *192*, 76-81.

[34]   M. Palomino, A. Corma, F. Rey, S. Valencia, *Langmuir* **2010**, *26*, 1910-1917.

[35]   I. Tiscornia, S. Valencia, A. Corma, C. Téllez, J. Coronas, J. Santamaría, *Microporous Mesoporous Mater.* **2008**, *110*, 303-309.

[36]   M. Miyamoto, Y. Fujioka, K. Yogo, *J. Mater. Chem.* **2012**, *22*, 20186-20189.

[37]   H. Maghsoudi, M. Soltanieh, H. Bozorgzadeh, A. Mohamadalizadeh, *Adsorption* **2013**, *19*, 1045-1053.

[38]   A. Huang, J. Caro, *Chem. Commun.* **2010**, *46*, 7748-7750.

[39]   D. H. Olson, M. A. Camblor, L. A. Villaescusa, G. H. Kuehl, *Microporous Mesoporous Mater.* **2004**, *67*, 27-33.

[40]   N. Hedin, G. J. DeMartin, W. J. Roth, K. G. Strohmaier, S. C. Reyes, *Microporous Mesoporous Mater.* **2008**, *109*, 327-334.

[41] R. Krishna, J. M. van Baten, *Microporous Mesoporous Mater.* **2011**, *137*, 83-91.

[42] A. Corma, F. Rey, J. Rius, M. J. Sabater, S. Valencia, *Nature* **2004**, *431*, 287-290.

[43] I. Daems, R. Singh, G. Baron, J. Denayer, *Chem. Commun.* **2007**, 1316-1318.

[44] J. F. A. Denayer, L. I. Devriese, S. Couck, J. Martens, R. Singh, P. A. Webley, G. V. Baron, *J. Phys. Chem. C* **2008**, *112*, 16593-16599.

[45] T. Remy, J. C. Saint Remi, R. Singh, P. A. Webley, G. V. Baron, J. F. M. Denayer, *J. Phys. Chem. C* **2011**, *115*, 8117-8125.

[46] J. Cousin Saint Remi, G. V. Baron, J. F. M. Denayer, *J. Phys. Chem. C* **2013**, *117*, 9758-9765.

[47] A. F. Cosseron, T. J. Daou, L. Tzanis, H. Nouali, I. Deroche, B. Coasne, V. Tchamber, *Microporous Mesoporous Mater.* **2013**, *173*, 147-154.

[48] M.-J. Diaz-Cabanas, P. A. Barrett, *Chem. Commun.* **1998**, 1881-1882.

[49] R. L. Gorring, *J. Catal.* **1973**, *31*, 13-26.

[50] H. Wu, Q. Gong, D. H. Olson, J. Li, *Chem. Rev.* **2012**, *112*, 836-868.

[51] V. Bolis, C. Busco, P. Ugliengo, *J. Phys. Chem. B* **2006**, *110*, 14849-14859.

[52] M. Trzpit, M. Soulard, J. Patarin, N. Desbiens, F. Cailliez, A. Boutin, I. Demachy, A. H. Fuchs, *Langmuir* **2007**, *23*, 10131-10139.

[53] J. Cousin-Saint-Remi, J. F. M. Denayer, *Chem. Eng. J.* **2017**, *324*, 313-323.

[54] R. Krishna, J. M. van Baten, *Langmuir* **2010**, *26*, 10854-10867.

[55] Q. Qian, J. Ruiz-Martínez, M. Mokhtar, A. M. Asiri, S. A. Al-Thabaiti, S. N. Basahel, B. M. Weckhuysen, *Catal. Today* **2014**, *226*, 14-24.

[56] A. Galadima, O. Muraza, *Ind. Eng. Chem. Res.* **2015**, *54*, 4891-4905.

[57] Y. Chen, Y. Wu, L. Tao, B. Dai, M. Yang, Z. Chen, X. Zhu, *Journal of Industrial and Engineering Chemistry* **2010**, *16*, 717-722.

[58] Y. Hirota, Y. Nakano, K. Watanabe, Y. Uchida, M. Miyamoto, Y. Egashira, N. Nishiyama, *Catal. Lett.* **2012**, *142*, 464-468.

[59] Y. Li, M. Zhang, D. Wang, F. Wei, Y. Wang, *J. Catal.* **2014**, *311*, 281-287.

[60] M. Salmasi, S. Fatemi, S. J. Hashemi, *Scientia Iranica* **2012**, *19*, 1632-1637.

[61] X. Zhang, R. Wang, X. Yang, F. Zhang, *Microporous Mesoporous Mater.* **2008**, *116*, 210-215.

[62] J. Jänchen, D. Ackermann, E. Weiler, H. Stach, W. Brösicke, *Thermochim. Acta* **2005**, *434*, 37-41.

[63] A. Faisal, M. Zhou, J. Hedlund, M. Grahn, *Adsorption* **2016**, *22*, 205-214.

[64] V. Saravanan, D. A. Waijers, M. Ziari, M. A. Noordermeer, *Biochemical Engineering Journal* **2010**, *49*, 33-39.

[65] X. Lin, J. Wu, X. Jin, J. Fan, R. Li, Q. Wen, W. Qian, D. Liu, X. Chen, Y. Chen, J. Xie, J. Bai, H. Ying, *Biotechnol. Prog.* **2012**, *28*, 962-972.

[66] J. Cousin Saint Remi, A. Lauerer, C. Chmelik, I. Vandendael, H. Terryn, G. V. Baron, J. F. M. Denayer, J. Karger, *Nat. Mater.* **2016**, *15*, 401-406.

[67] G. Kresse, J. Furthmüller, *Physical Review B* **1996**, *54*, 11169-11186.

[68] G. Kresse, D. Joubert, *Physical Review B* **1999**, *59*, 1758-1775.

[69] S. Grimme, S. Ehrlich, L. Goerigk, *J. Comput. Chem.* **2011**, *32*, 1456-1465.

[70] T. R. C. Van Assche, T. Duerinck, S. Van der Perre, G. V. Baron, J. F. M. Denayer, *Langmuir* **2014**, *30*, 7878-7883.

[71] V. Finsy, H. Verelst, L. Alaerts, D. De Vos, P. A. Jacobs, G. V. Baron, J. F. M. Denayer, *J. Am. Chem. Soc.* **2008**, *130*, 7110-7118.

Entry for the Table of Contents

Layout 1:

FULL PAPER

The production of biobutanol from fermentation solutions is afflicted by high separation costs due to the presence of co-products and a low final concentration. An alternative downstream process for butanol removal from a fermenter's head space is proposed via a specific 2-stage adsorptive method which couples very high product recovery to an extremely high purity.
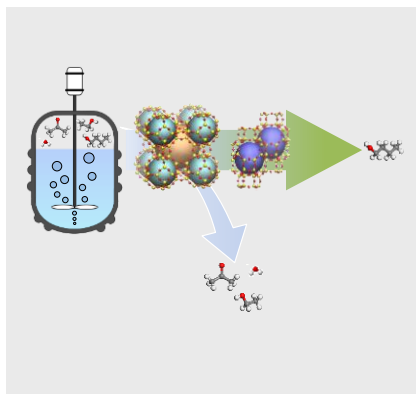
S. Van der Perre, P. Gelin, B. Claessens, A. Martin-Calvo, J. Cousin Saint Remi, T. Duerinck, G.V. Baron, M. Palomino, L.Y. Sánchez, S. Valencia, J. Shang, R. Singh, P.A. Webley, F. Rey, J.F.M. Denayer*

Page No. – Page No.

Intensified biobutanol recovery using zeolites with complementary selectivity

Author/s:

Van der Perre, S; Gelin, P; Claessens, B; Martin-Calvo, A; Saint Remi, JC; Duerinck, T; Baron, GV; Palomino, M; Sanchez, LY; Valencia, S; Shang, J; Singh, R; Webley, PA; Rey, F; Denayer, JFM

Title:

Intensified Biobutanol Recovery by using Zeolites with Complementary Selectivity

Date:

2017-07-21

Persistent Link:

http://hdl.handle.net/11343/293151

File Description:

Accepted version